A MANFIS model of the 3D head position based on a wearable system

Dan-Marius DOBREA and Monica-Claudia DOBREA

Electronics, Telecommunications and Information Technology, "Gheorghe Asachi" Technical University,
Iași, România
E-mails: mdobrea@etti.tuiasi.ro, mcdobrea@etti.tuiasi.ro

Abstract. The fuzzy systems, the artificial neural networks, and the neuro-fuzzy systems have been widely used in modeling of the complex, unknown and nonlinear functions. In this paper, a comparative study between two soft computing techniques was done, namely, between: (a) a *Multiple Neuro-Fuzzy Inference System* (MANFIS) and (b) two different Artificial Neural Network structures - and this comparison was one investigated in relation with a practical embedded application. More precisely, the research used a new wearable system, named ***Intell.TieSens***, in order to model the complex nonlinear relationship that exist between the capacitive sensors embedded in a tie collar and the 3D head position of the wearer of that tie. The ***Intell.TieSens*** system was designed to be a noncontact system, low power, portable, lightweight, having a Bluetooth Low Energy wireless data communication capability in order to be able both to be paired with a personal computer or with a smartphone and to identify in real time the human 3D head position. The results showed the superior performances obtained with MANFIS system – two times better than the performances obtained with the RBF (*Radial Basis Function*) neural network. Out of the tested models, the MLP (*MultiLayer Perceptron*) neural network obtained the lowest performances.

Key-words: Fuzzy, MANFIS, CANFIS, neural network, RBF, wearable, capacitive sensing.

1. Introduction

The function approximation problems concerns in the estimation of an unknown model with simpler functions using for this information extracted from pairs of known input-output samples. The final goal of the constructed model is to obtain the correct output value when a new input data is used. However, many times in practical situation, the deep knowledge regarding the biological processes or the existing knowledge about different plant models are not enough to extract equations of the mathematical model of the unknown system. In such situation, the solution is to

obtain many statistical representative input-output data, from the unknown, model and to use a neuro-fuzzy or artificial neural network (ANN) system to model the unknown behavior.

The artificial neural networks and the fuzzy systems [1], each of them with its advantages as well as with its disadvantages, have been widely used in modeling of unknown nonlinear processes or in optimal control [2]. In addition, the integration of neural networks and fuzzy logic systems generated a new class of neuro-fuzzy systems that combine the advantages of both ANN and fuzzy logic in a new framework.

The neuro-fuzzy systems has been applied with success in many fields of engineering and science, including: dynamic system identification [3, 4], filtering [5], mechanical property prediction [6], economy [7], brain tumor detection [8], motor model and control [9, 10], sensors [11], fault diagnosis [12], etc.

Having in mind the results reported so far in the literature, this paper proposes to find the best solution for modeling the unknown relation that exist between four capacitive sensors placed around the neck of a subject - sensors that are embedded into a tie collar - and the subject's head position. Such a system can prove to be very useful, having many potential applications like: detection and assessment of the epilepsy seizures [13], identification of the body postures [14], health monitoring [15] or human activity recognition [16].

2. The wearable system

Intell.TieSens is a new wearable capacitive sensor system able to monitor, without any contact, people performing their usual tasks. The final goal of this system is to correctly identify the 3D head position of a subject in real time and in a real environment.
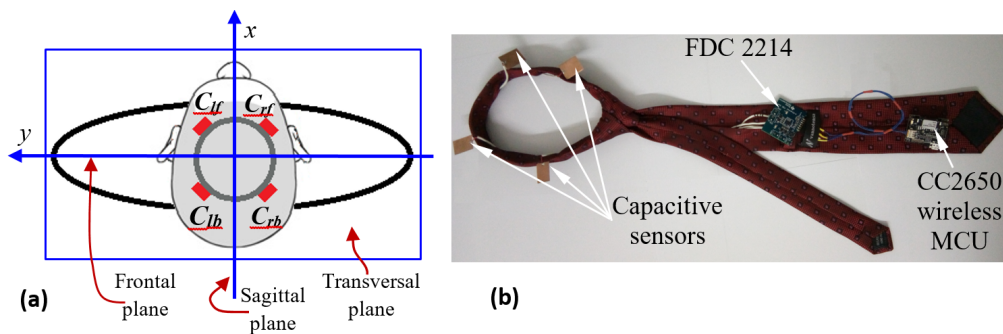
Fig. 1. (a) The sensors measuring setup and (b) The Intell.TieSens system.

2.1. Measuring setup

The *Intell.TieSens* system is based on the information obtained from four capacitive sensors (C_{lf}, C_{lb}, C_{rb}, and C_{rf}), placed around the neck (see Figure 1(a)). Based on these sensors it performs a measurement of the head position. The system is able to detect the rotation of the head around (Figure 1(a) and (b)): yaw axis (head rotation in the transversal plane), pitch axis (the rotation of the head in the sagittal plane) and the roll axis (head rotation in the frontal plane). The Intell.TieSens uses only the measurement values of these capacitors to identify the 3D the head position and movements.

The values of the sensors, (C_{lf}, C_{lb}, C_{rb}, and C_{rf}), are in a direct relation with the subject head position. As a result, a complex movement (that took place simultaneously in all the axes) will be reflected, as information, in all four sensors. For example, in Figure 2, the capacitive signals for a continuous motion of the head in the transversal plane is presented: the head orientation goes from 0° position to –45° position to the left; then, it returns to the initial state, the 0-degree position, and continues to the right, until the +45° position is reached. In the end, it returns to the 0-degree position. In Figure 2 the specific mean values were extracted from the signals of all channels. The relationship between the sensor values and the head movement will be further presented, in detail, in subchapter 3.1 of this paper.

An extensive, comparative analysis of **Intell.TieSens** system with other similar systems was done in [31]. In summary, we highlight here the main differences between Intell.TieSens and other systems proposed in the literature [31]: (a) the other referred systems have dedicated sensors to sense each particular motion [17, 18, 19], (b) the placement of the sensors follows other configurations than in our case, (c) the other systems combine different types of sensors: capacitive, resistive, inductive and bio-impedance and (d) another main difference consists in the measurement system itself - in the present research, a narrow-band LC-based capacitive measurement system was used. The system proposed by us does not follow these approaches. This fact will generate a software complexity, due to the implied methods required in the extraction and identification of a specific head position based on the mixed information generated by the sensors.
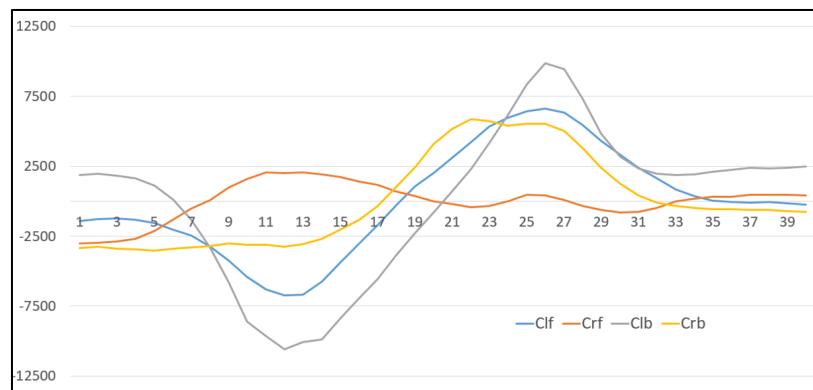
Fig. 2. The response of sensors, obtained for head movement in the transversal plan.

2.2. The hardware system

The wearable system is built around a SimpleLink CC2650 wireless System-on-Chip (SoC) device, produced by Texas Instruments Company. SimpleLink CC2650 SoC is, mainly, composed of three different processors (see Figure 3): (a) a Cortex-M0 processor that manages the physical layer of the Bluetooth 2.4 GHz RF transceiver embedded on the chip, (b) a Cortex-M3 processor that handles the user application and the upper layers of the BLE (Bluetooth Low Energy) protocol, and (c) an ultra-low-power Sensor controller engine (SCE) that manages, in our case, only the external driver circuit (FDC2214) for the capacitive sensor.
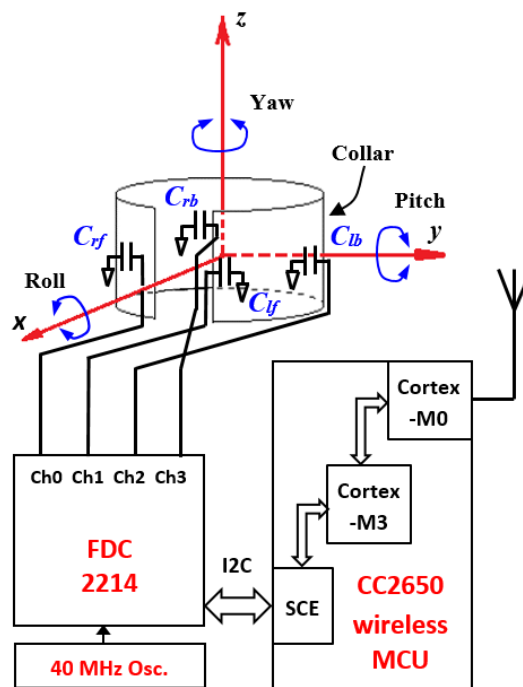
Fig. 3. The *Intell.TieSens* system block diagram.

2.3. The software components

In order to get an operational *Intell.TieSens* system, two applications were developed: (1) one, at the wearable system level (i.e, deployed on the CC2650 SoC), and (2) another one–a Windows 10 application–, was designed to interact with the wearable system. From the software point of view, the wearable device works as a GATT (Generic Attribute Profile) server. Consequently, a corresponding client application had to be provided in order to communicate with it.

The first above-mentioned component, which runs on the CC2650 SoC processor, is primarily responsible for the control as well as for data exchange functions through the BLE protocol. To achieve these goals a new GATT (Generic Attributes) service and four new characteristics were implemented. The characteristics were especially designed in order: (a) to activate a specific data acquisition channel, (b) to set the sensor measurement period (*i.e.*, from 120 ms up to 2550 ms), and (c) to receive the data - from the Ch0 and Ch1 channels (the third characteristic) and from the Ch2 and Ch3 channels (the last characteristic).

The second component, running on Windows 10 operating system, is used to: configure, interrogate, get capacitive data, save this data (to an Excel sheet, or to a text file) and present it to the user in text or graphical format. To implement all these functionalities an existing application named *blessTags*, was completed with new modules.

The *blessTags* application is a program that can manage, set, communicate, use and display information from five different types of SensorTags – examples with some of this software's user-interfaces are given in Figure 3. The blessTags application [20] is commercialized within

the virtual Microsoft Store and it was developed by the first author of this paper. In this research, the ***blessTags*** package offers basic support for the BLE protocol communication.
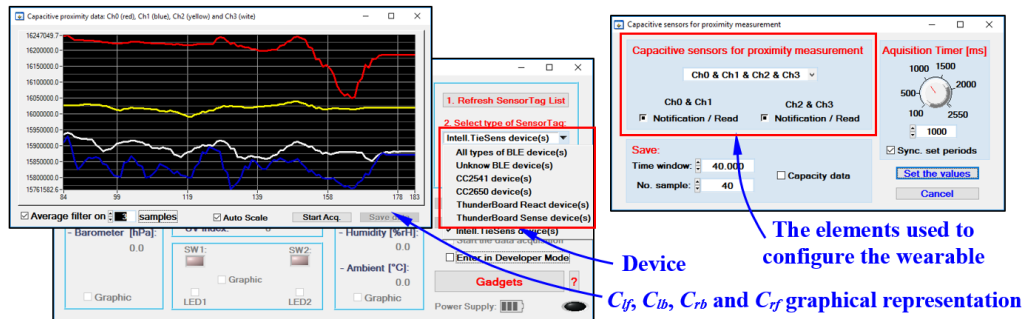
Fig. 4. The blessTags application with some of its different user-interfaces.

3. The neuro-fuzzy model of the 3D head position

3.1. The model complexity

For the problem, presented in this paper, the sensor capacitance changes proportionally with: (a) the properties of the dielectric materials of the human body tissues that compose the area localized underneath the sensor (i.e., the neck, in our case), as well as with (b) the shapes and movements of the neck's different constituent tissues (*i.e.*, skin, muscles, tendons, blood vessels etc.).

The sensitivity of the capacitive sensors varies in direct relation with the dielectric constant of the target to measure. The dielectric constant of a biological tissue depends on the organic and inorganic constituents of that tissue, from both cellular and molecular levels. The larger is the value of the dielectric constant of a material (a specific tissue), the easier is to detect it. For a particular tissue, the dielectric parameters are mainly dependent on its water content. The water dielectric constant is about 80. The capacitance of a body tissue increases with the increasing water content, which, in turn, is known as fluctuating with the moment of the day, the hydration, the body temperature, the physical effort, the emotional state etc. In addition, there are other individual's specific factors which exert great influence on the electrical properties of a living tissue [21, 22, 23, 24]. Such factors are: (a) the ions that are suspended in water, (b) the ionic diffusion through the cellular membrane, (c) the polarization of the cell membranes, (d) the polarization of the water molecules and (e) the gradient of the water content related with the depth under the skin surface.

There is a large number of muscles involved in head orientation [25]. Several of these muscles are [25]: the sternocleidomastoid (used in abduction, adduction, extension, flexion, and rotation of the neck), platysma (involved in the left and right motion commands), the trapezius (for upwards motion commands), splenius (used to rotate and extend the head and the neck), iliocostalis, longissimus and spinalis (all three used to extend and to flex the control abduction and adduction of the spine and neck). By using all these muscles and many others, human succeeds to move his head in any wanted direction according to the specific movement command given by the brain to the neck muscles. These muscles work both individually as well as in pairs (placed on the left and right sides of the neck), with the final goal to rotate the head and to flex the neck.

The muscles presented above, together with other tissues represents the dielectric components for the capacitive sensors placed around the neck, see Figure 1(a) and (b) and Figure 2. Based on these dielectrics, the capacitive sensors are mapping, into a specific set of values, each orientation of the head. The final goal of our research consists in finding the relationship established between the capacitive sensor values and the actual direction of the individual head orientation. Due to the variabilities and specificities of the human tissues, this is not a trivial task.

In order to sense the head position, one can embed the capacitive electrodes either in a shirt collar or in a necktie (as in our case, see Figure 1(b)). In this way, the sensors have no direct contact with the body. Namely, the capacitive electrodes are separated by the body through a barrier – a textile layer. More, because the tissues of the neck have a much higher dielectric value than the surrounding textile layers (for example, the dielectric constant for different materials are: 1.3 ÷ 1.4 for cotton; 2.8 ÷ 5.2 for different types of polyester fibers, 2.7 ÷ 4.5 for the acrylic fibers, which are used to imitate wool; 4.0 ÷ 5.0 for the nylon fibers, that are used to imitate silk etc.), the sensor proved to have the ability to "see through" the textile and, consequently, to detect the neck movements.

3.2. Function approximation

Due to the very complicated and unknown relation, that exists between the capacitance values (C_{lf}, C_{lb}, C_{rb}, and C_{rf}) and the head orientation (yaw-pitch-roll angles):

$$\alpha_i = f_i(C_{lf},\ C_{lb},\ C_{rb},\ C_{rf}),\ \ i = \overline{yaw, pitch, roll} \tag{1}$$

in what follows, specific nonlinear functions (for each of the 3D axes) are going to be found starting from the input-output data set recorded previously. For this, the mean value was extracted from the values of each channel (C_{lf0}, C_{lb0}, C_{rb0}, and C_{rf0}); in this mode, the effect generated by the parasitic values introduced by the shiftings in the distance between the sensor and the skin was reduced. At the inputs of the system used to model the fi functions – see (1), only the four capacitive values – C_{lf0}, C_{lb0}, C_{rb0}, and C_{rf0} – were supplied.

The universal approximation theorem states that a neural network or a fuzzy system (if they obey some conditions [2], [26]) can approximate a real function, like (1), with an arbitrarily small error ε:

$$|f_i(x) - \widehat{f}_l(x, w)| < \varepsilon,\ \ \ x = [C_{lf0}, C_{lb0}, C_{rb0}, C_{rf0}]^T \tag{2}$$

In (2) the $\widehat{f}_i$ function is an approximation of f_i function. The goal is to find a particular set of w_i coefficients able to obey relation (2), for each function f_i, using for this a combination of elementary functions $\varphi_i(x)$ such as:

$$\widehat{f}_i(x, w) = \sum_{i=1}^{N} w_i \cdot \varphi_i(x) \tag{3}$$

The main factors required to get the smallest approximation error ε are: (a) finding the appropriate type of φ_i function, (b) finding the optimum number N of the elementary functions and (c) finding the best weights w_i.

One of the most important steps, with a huge impact on the quality of the approximation, is the choice of the elementary functions – the φ_i functions. In order to find the most accurate

approximation of the functions f_i, we decided to use several distinct models, based on several different types of elementary functions and, at the end, to choose the best one of them. For this reason, we chose and implemented the following models: multilayer perceptron, RBF (Radial Basis Function) neural network and MANFIS (Multiple Adaptive Neuro-Fuzzy Inference System).

3.3. The neuronal models

Two types of neural networks, MLP (multilayer perceptron) and RBF (radial basis function) were used in this research. We chose these neural networks mainly because they embed within their structure different types of elementary functions (φ_i), with different types of properties.

Mostly, in classification as well as in function approximation applications, the MLP model uses sigmoidal types of nonlinearities (*i.e.*, logistic or tangent hyperbolic functions). These ones are global elementary functions, because they respond to the entire input space. During the training phase, this type of neural network structure changes - according to the training data - its elementary functions position, slope, and, thus, as a direct consequence, the functions composition itself. As a result, over time, the approximation of f_i function becomes better and better.

The RBF network is an alternate topology used intensively in function approximation. This network uses another type of elementary functions, namely, the localized radial basis functions (φ_i). Even if the RBF networks are universal approximators, [27], like in the MLP network case, selecting the network parameters proves to be not a trivial task.

3.4. The ANFIS model

The third model used in this research is based on a fuzzy inference system. The fuzzy systems are a very powerful tool in function approximation due to the flexibility in linguistic control, which is essentially based on the if-then rule set. However, this type of systems has its own drawbacks. The main problem of such systems is given by the difficulty encountered in determining the shape and the location of each membership function for each fuzzy input variable. To solve this problem, an ANFIS (Adaptive Neuro-Fuzzy Inference System) model is used. The ANFIS integrates adaptable fuzzy inputs with a modular neural network in order to approximate complex functions.

The implemented ANFIS model uses a first order Sugeno fuzzy model. In our case, for a system with four input variables, the fuzzy if-then rules database can be expressed as:

$$Rule\ k: If\ x\ is\ A_3\ and\ y\ is\ B_2\ and\ z\ is\ C_2\ and\ v\ is\ D_1$$
$$then\ o_k = p_k x + q_k y + r_k z + s_k v + t_k \tag{4}$$

In (4) A_i, B_i, C_i and D_i (with $i = 0, 1, 2$ in our case) are the fuzzy sets for the inputs x, y, z, and v, respectively; p_k, q_k, r_k, s_k and t_k are the parameters in the consequent part of the k rule and they are determined during and based on the training process.

The architecture of the implemented ANFIS model is presented in Figure 5. Five layers compose the ANFIS architecture [28]. Each layer has nodes with similar functions.

The nodes in Layer 1 are all adaptive, with a node output function of:

$$
\begin{aligned}
O_{1,j} &= \mu_{A_j}(x) & j &= \overline{0,2} \\
O_{1,k+3} &= \mu_{B_k}(y) & k &= \overline{0,2} \\
O_{1,l+6} &= \mu_{C_l}(z) & l &= \overline{0,2} \\
O_{1,m+9} &= \mu_{D_m}(v) & m &= \overline{0,2}
\end{aligned} \tag{5}
$$

The outputs of the first layer specify in which degree the given inputs ($x = C_{lf0}$, $y = C_{lb0}$, $z = C_{rb0}$, and $v = C_{rf0}$) satisfy the corresponding quantifiers (A_i, B_j, C_k or D_l). We use for each input three membership functions (MF). The optimal number of MF was determined within a process of trial-and-error type. The approximation error was tested for 2, 3, 4 and 5 fuzzy sets, for inputs x, y, z and v. For our problem, the best results were obtained for using three fuzzy sets on each input. Each fuzzy set is defined by a specific membership function – in our research, the ANFIS implementation and tests were done using the Gaussian and generalized bell membership function types. The parameters of the membership functions are referred in the scientific literature as the premise parameters [28].

The Layer 2 of the ANFIS model receives inputs from the first layer, and computes the product of all output pairs from the first layer, in the form given below:

$$
O_{2,i} = w_i = \mu_{A_j}(x) \cdot \mu_{B_k}(y) \cdot \mu_{C_l}(z) \cdot \mu_{D_m}(v) \qquad i = \overline{0,80} \tag{6}
$$

These outputs represent the strengths of the corresponding fuzzy rules. Having four inputs, and, more, for each of the input variables having three linguistic terms, we come to the situation in which a maximum of 3 x 3 x 3 x 3 = 81 possible combinations is obtained. Further, this calculus translates into the fact that on the second layer a number of 81 nodes will be derived.

Like the elements of Layer 2, the elements from Layer 3 are, also, fixed nodes. These nodes calculate a normalized firing strength, according to the following formula:

$$
O_{3,i} = \overline{w}_i = \frac{w_i}{\sum_{j=1}^{81} w_j} \qquad i = \overline{0,80} \tag{7}
$$

Unlike the two previous layers, the Layer 4 is one composed of adaptive elements. The output function for each of its nodes is given by:

$$
O_{4,i} = \overline{w}_i f_i = \overline{w}_i \left(p_i x + q_i y + r_i z + s_i v + t_i \right) \qquad i = \overline{0,80} \tag{8}
$$

Here, the p_i, q_i, r_i, s_i and t_i are the parameters for the i node, parameters that will be adapted in order to decrease the approximation error. These parameters are referred to as the consequent parameters.

The last layer computes the outputs as a sum of all its inputs:
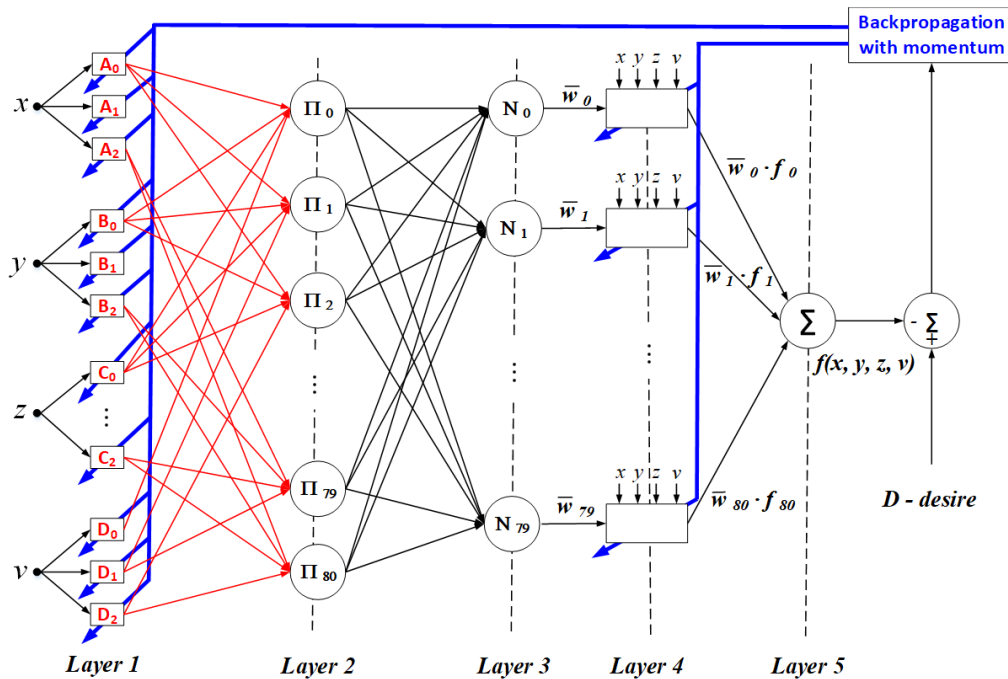
Fig. 5. The architecture of ANFIS with four inputs, three linguistic labels for each input and one output.

The ANFIS model has the disadvantage of modeling only one unknown function. However, in our case, the modeling system expects three outputs: an output for each angle of the head position corresponding to: yaw, pitch, and roll.

There are at least two ways to obtain a system with multiple outputs, starting from the ANFIS model. An easy way to accomplish this consists in placing several ANFIS systems in parallel, and feeding them with the same inputs, but with different outputs. Such a system is known in the literature as the MANFIS model – multiple ANFIS. In another approach, the ANFIS models can be designed as having the same antecedents of fuzzy rules sets – this means that, all the constituent ANFIS systems are going to have as identical all the first three layers, see Figure 5. The next two layers are, however, designed to be specific for each of the ANFIS systems. This new type of neuro-fuzzy systems is called CANFIS (Coactive Neuro-Fuzzy Inference Systems).

4. Estimating the head angles in 3D space

4.1. Database recording

Three subjects, two females (of age 22 and 42), and a male (44 years old), participated to this study. The subjects sat on a chair, with their backs supported by the deck of the chair. Over the entire recording time, the subjects kept their torsos in a vertical position. The chair was placed at halfway between the two lateral walls (i.e., the subject's left and right side).

In order to make measurements for the head rotation in both the transversal and sagittal planes, on all three walls (left, right and front walls) different landmarks were placed in line,

at equal distances (*i.e.*, from 5 to 5 degrees). Therefore, on the front wall, the landmarks were placed in the vertical position, at the intersection line between the subject sagittal plane and the front wall, starting with –60° and ending with +60° vertical angle in the subject's sagittal visual field, see Figure 6(a). In this mode, the subject head pitch angle was measured. In a similar way, in order to measure the exact yaw angle of the head, a grid of points was spread on an imaginary line placed in transversal plane, over the all three walls (*i.e.*, the left, frontal, and right wall). At its turn, the subject's head roll angle was measured in the frontal plane by placing some landmarks on the frontal wall, as they are indicated in Figure 6(b).

The data sets recorded in this study were obtained as follows: each participant to the study was asked to look at a particular landmark indicated via a voice command. For each such landmark, six distinct measurements were acquired in a random order, being interleaved with measurements corresponding to other angles. To ensure a reproducible measurement, a laser pointer (LP) was mounted on a helmet placed on the subject's head, Figure 6(b). The laser pointer was placed either at the subject eyes level - for the measurements in the sagittal plane -, or on the top of the helmet – for the measurements in the transversal and frontal planes. In all cases the LP pointed in the subject's ahead direction. Also, the participants were asked to hold the laser pointer on the specified landmark until the next command was issued.
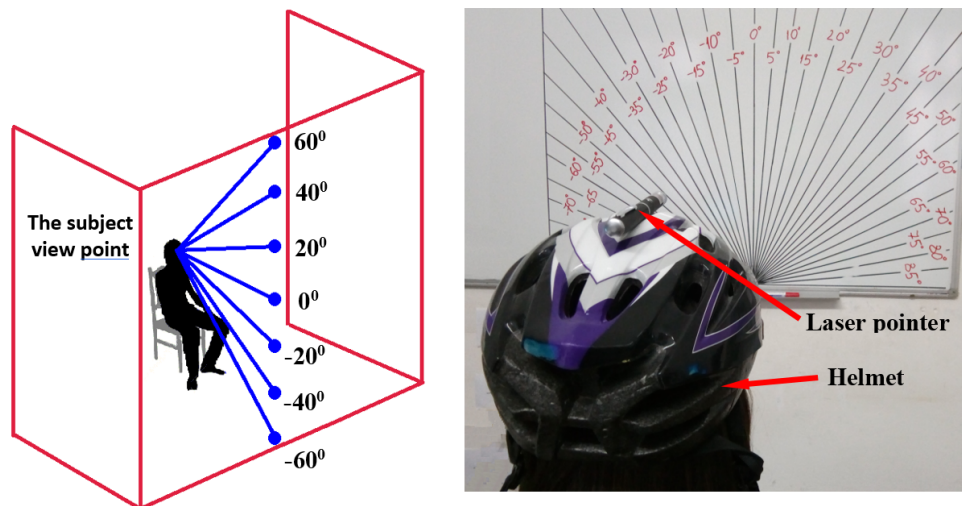
Fig. 6. The placement of the landmarks on the walls for: (a) sagittal angles and (b) frontal angles – roll head angle.

Following the above recording paradigm, the training data sets for the MANFIS model and for the neuronal networks were obtained. The data sets consisted in the input values (*i.e*, the capacitive sensors values) and in the corresponding outputs values (*i.e.*, the subject's head positions). During data acquisition process some unexpected aspects were encountered, with all these related to the extreme values of the pitch, roll and yaw angles. Namely, not all users had the physical capacity to express them. That is why, at the end, only 1618 data were acquired and used to train the models.

4.2. Performance metrics

The performances for the fuzzy model and for both neuronal structures, used in this study, were evaluated with four different metrics: the mean squared error (MSE), the normalized mean squared error (NMSE), the correlation coefficient (r), and the percent error ($\%_{error}$).

The MSE error incorporates both: (a) the variance of the model estimator (how widely are spread the estimates) and (b) its bias (how far the average estimated model is from the real value). So, to establish how well the model output fits the desired output we used the MSE and the NMSE errors. Nevertheless, MSE and NMSE does not reflect whether the two modeled sets of data move in the same direction or not. To eliminate this shortcoming, we computed in addition the correlation coefficient. The last parameter, the percent error, was computed in the following way:

$$\%_{error} = \frac{100}{N} \sum_{i=0}^{N-1} \left| \frac{dy_i - dd_i}{dd_i} \right| \tag{9}$$

where: d_{yi} is the denormalized model output for exemplar i, d_{di} is the denormalized desired output and N is the number of exemplars on which the percent error was computed. Unfortunately, this parameter can easily be misleading. For example, in the case of an output data range of [–90°, +90°] – the case of the transversal plane head rotation - for an error of +5° instead of a real value of 5°, the percent error (%error) will be of 100 (hence, a huge error). However, for a value of 90°, the same obtained error of the model, of only +5°, will generate a percent error of only 5.55.

4.3. Results

With all models presented here, from the entire database we have used 80% for the training set and 20% of data for the cross-validation (CV) set. The performances presented in all the following tables were determined on the CV data set. In the preprocessing step, the training data set and the CV data set - more exactly, the inputs and the outputs values to the models - were previously normalized to the [–0.9, 0.9] interval.

Table 1. Neural network modeling performances for head rotation around each axes

Head angle	ANN type	MSE	NMSE	r	%error
Yaw	MLP (15)	0.0562	0.199	0.894	62.15
	RBF (45)	0.0436	0.154	0.920	52.66
Pitch	MLP (13)	0.0772	0.2	0.852	73.27
	RBF (42)	0.0490	0.168	0.975	54.19
Roll	MLP (12)	0.0586	0.207	0.89	60.91
	RBF (43)	0.0521	0.184	0.903	54.58

The performances obtained with the MLP and RBF networks are presented in Table I. All tested MLP artificial neural networks were composed of tangent hyperbolic neurons on the hidden layer, and of a linear neuron on the output layer. The backpropagation algorithm was used in order to train the MLP networks. For the RBF artificial neural network, we used, during the unsupervised learning stage (which lasted 100 epochs), the conscience full competitive rule with Euclidean metric.

In Table I, one can find the information regarding the number of the neurons used in the NN's hidden layer, as being written immediately after the network name, within parentheses. In the designing process of the neural networks, the optimal structure (the appropriate number of: (a) neurons in the first hidden layer for MLP network and (b) the radial based function for RBF network) was found by a trial-and-error method, based on Rissanen's minimum description length (MDL) criterion [26, 29]. For each head angle (*i.e.* yaw, pitch and roll) a specific artificial neural network model was used, with four inputs and one single output.

From Table I, one can see that the correlation coefficient is higher than 0.85 for the MLP networks and higher than 0.9 for the RBF networks. Both types of results suggest the same idea, namely, the fit of the model to the data is a very good one. Moreover, the RBF networks outperform the MLP networks performances in all tested cases, their MSE error being constantly lower than the error obtained with the MLP neural networks.

The architectures of neuro-fuzzy models were designed with: Gaussian membership function, Takagi-Sugeno-Kang fuzzy model, and backpropagation with momentum learning algorithm – see Figure 5. Each input variable had three linguistic terms.

The performances of the ANFIS model depend on two main factors: (a) on the membership function distributions of the input variables (*i.e.*, the premise parameters) and (b) on the coefficients (p_i, q_i, r_i, s_i and t_i, see equation (8)) of the first-order Takagi–Sugeno fuzzy system (*i.e.*, the consequent parameters). The modeling performances presented in Table II suggest that, for our problem, the optimum values were achieved when the membership functions were selected as being specifics to each modeled output angle (yaw, pitch, and roll). One direct consequence of this fact was: the MANFIS neuro-fuzzy model obtained better performances than the CANFIS neuro-fuzzy model. More than that, by comparing the results presented in Table I and Table II, one can easily notice that the MANFIS model obtained two times better performances than the RBF model.

Table 2. The modeling performances of MANFIS and CANFIS neuro-fuzzy structures

Head angle	Neuro-fuzzy model	MSE	NMSE	r	%error
Yaw	MANFIS	0.0268	0.0935	0.952	41.4
	CANFIS	0.0394	0.388	0.787	20.27
Pitch	MANFIS	0.0285	0.0979	0.936	46.73
	CANFIS	0.0394	0.388	0.787	20.27
Roll	MANFIS	0.0217	0.0834	0.967	38.52
	CANFIS	0.0394	0.388	0.787	20.27

The percent error (%error) for the CANFIS system, see Table II, is around 42. For a transversal plane head rotation from -90° up to +90° and a constant real error of only +5°, for each determination we will get a percent error (%error) equal with 100 for a desired value of 5° and an error of only 5.55 for a desired value of 90° - as we previously revealed. Knowing that the measurements were done from 5 to 5 degrees, the global mean percent error will be, in this case, of 52.775. However, the MANFIS modeling system obtained a percent error %error) of around 42. This primarily means that the MANFIS system obtains a mean approximation error of less than 5° - this is also our resolution used for the database recording. The CANFIS performances, see Table II, are the same for each head rotation (yaw, pitch, and roll) because the structure of this modeling system has four inputs and three outputs, and it is not composed of three different ANFIS systems like in the case of MANFIS system. For CANFIS system the modeling

performances are computed globally for all head rotation angles.

The structure of MANFIS model is more complicated than the structure of both neural networks models (MLP and RBF neural networks), due to a larger number of free terms that should be determined from the data to be modeled, within the applied adaptation algorithm. In addition, the training time of MANFIS models takes longer (around 17000 epochs) compared to the equivalent training time needed by the neural network structures (around 6000 epochs). On the other hand, the accuracy level of MANFIS model is much better than the one of neuronal networks (at least two time superior). As a conclusion, MANFIS architecture proved to be a better approach when modelling the nonlinear relationship between the capacitances values and the subject's 3D head position.

5. Conclusions

The research presented in this paper continues the researches presented in [30] and [31]. The paper discusses three different approaches that could be considered for modelling the complex relationships that exist between the capacitance values measured from four sensors embedded within a tie collar and the head direction information of the subject that is wearing that tie. After studying this complex and nonlinear relationship, we first concluded that it is too complicated to provide a mathematical model for it. As a result, two neuronal models (a MLP network and a RBF network) and two neuro-fuzzy models (MANFIS and CANFIS) were further considered, designed, implemented and analyzed.

From the results reported above we draw the following conclusion: modeling the complex and nonlinear relationship that exists between the capacitive sensors values (*i.e.*, sensors placed around the neck as in Figure 1(a) and Figure 3), and the head 3D position by using a MANFIS model proved to deliver a better accuracy than when modeling the same relationship with a MLP or with a RBF artificial neural network. Therefore, the MANFIS model should be considered for use in the future with the ***Intell.TieSens*** wearable system.

References

[1] Zadeh L.A., *Fuzzy Sets, Information and Control*, **8**, 1965, pp. 338–353.

[2] Teodorescu H.N., *On Zadeh's Contribution to the Optimality Problem: Four Points of View on Optimality – Logic, Set Theory, Theory of Uncertainty, and Analytic*, Romanian Journal of Information Science and Technology, **20**(3), 2017, pp. 179–184

[3] Haznedara B., Kalinli A., *Training ANFIS Structure Using Simulated Annealing Algorithm for Dynamic Systems Identification*, Neurocomputing, **302**, 2018, pp. 66–74.

[4] Zhang Y., Chai T., Wang H., Chen X., Su C.Y., *An Improved Estimation Method for Unmodeled Dynamics Based on ANFIS and Its Application to Controller Design*, IEEE Transactions on Fuzzy Systems, **21**(6), 2013, pp. 989-1005.

[5] Kimiaefar R., Siahkoohi H.R., Hajian A., Kalhor A., *Random Noise Attenuation by Wiener-ANFIS Filtering*, Journal of Applied Geophysics, **159**, 2018, pp. 453–459.

[6] Umrao R.K., Sharma L.K., Singh R., Singh T.N., *Determination of Strength and Modulus of Elasticity of Heterogenous Sedimentary Rocks: An ANFIS Predictive Technique*, Measurement, **126**, 2018, pp. 194–201.

[7] Jovic S., Miladinovic J.S., Micic R., Markovic S., Rakic G., *Analysing of Exchange Rate and Gross Domestic Product (GDP) by Adaptive Neuro Fuzzy Inference System (ANFIS)*, Physica A: Statistical Mechanics and its Applications, **513**, 2019, pp. 333–338.

[8] Selvapandian A., Manivannan K., *Fusion Based Glioma Brain Tumor Detection and Segmentation Using ANFIS Classification*, Computer Methods and Programs in Biomedicine, **166**, 2018, pp. 33–38.

[9] Krasopoulos C.T., Beniakar M.E., Kladas A.G., *Multicriteria PM Motor Design Based on ANFIS Evaluation of EV Driving Cycle Efficiency*, IEEE Transactions on Transportation Electrification, **4**(2), 2018, pp. 525-535.

[10] Fu Y., Yang H., Ding J., *Multiple Operating Mode ANFIS Modelling for Speed Control of HSEMU*, IET Intelligent Transport Systems, **12**(1), 2018, pp: 31–40.

[11] Sowmmiya U., Uma G., *ANFIS-Based Sensor Fault-Tolerant Control For Hybrid Grid*, IET Generation, Transmission & Distribution,**12**(1), 2018, pp. 31–41

[12] Fan J., Wang F., Sun Q., Bin F., Liang F., Xiao X., *Hybrid RVM–ANFIS Algorithm for Transformer Fault Diagnosis*, IET Generation, Transmission & Distribution, **11**(4), 2017, pp. 3637–3643.

[13] Villar J.R., Vergara P., Menéndez M., De La Cal E., González V.M., Sedano J., *Generalized Models for the Classification of Abnormal Movements in Daily Life and its Applicability to Epilepsy Convulsion Recognition*, International Journal of Neural Systems, **26**(6), 2016.

[14] Dobrea D.M., M.C. Dobrea, *A Warning Wearable System Used to Identify Poor Body Postures, Advances in Wireless and Optical Communications (RTUWO)*, Riga, Letonia, 2018.

[15] Pantelopoulos A., Bourbakis N.G., *A Survey on Wearable Sensor-Based Systems for Health Monitoring and Prognosis*, IEEE Transactions on Systems, Man, and Cybernetics, Part C (Applications and Reviews), **40**(1), 2010, pp. 1–12.

[16] Lara Ó.D., Labrador M.A., *A Survey on Human Activity Recognition Using Wearable Sensors,* IEEE Communications Surveys and Tutorials, **15**(3), 2013, pp. 1192–1209.

[17] Cheng J., Amft O., Lukowicz P., *Active Capacitive Sensing: Exploring a New Wearable Sensing Modality for Activity Recognition, in: Pervasive 2010*, LNCS 6030, P. Floreen, A. Kruger and M. Spasojevic, Eds. Springer-Verlag Berlin Heidelberg, 2010, pp. 319–336.

[18] Hagan M., and O. Geman, *A Wearable System for Tremor Monitoring and Analysis, Proceedings of the Romanian Academy - Series A: Mathematics*, Physics, Technical Sciences, Information Science, 17 (1), 2016, pp. 90–98.

[19] Cheng J., et al., *Textile Building Blocks: Toward Simple, Modularized, and Standardized Smart Textile, in: Smart Textiles*, Human–Computer Interaction Series, S. Schneegass and O. Amft, Eds., Springer, Cham, 2017, pp. 303–331.

[20] Dobrea D.M., *The blessTags application*, Microsoft Windows Store, https://www.microsoft.com/store/apps/9p054xsjjr1n.

[21] Ruan F., Dlugosz T., Shi D., Gao Y., *Cylinder Model of Human Body Impedance Based on Proximity Effect*, 3rd IEEE International Symposium on Microwave, Antenna, Propagation and EMC Technologies for Wireless Communications, 2009, Beijing, China, pp. 16–19.

[22] Yamamoto T., Yamamoto Y., *Analysis for the Change of Skin Impedance*, Medical and Biological Engineering and Computing, 1977, 15(3), pp. 219–227.

[23] Gabriel C., Gabriel S., Corthout E., *The Dielectric Properties of Biological Tissues: I. Literature survey*, 1996, Physics in Medicine & Biology, **41**, pp. 2231–2249.

[24] Moore K.L., Agur A.M.R., Dalley A.F., Clinically Oriented Anatomy, 8th Edition, Publisher Wolters Kluwer, 2018.

[25] Moore K.L., Agur A.M.R., Dalley A.F., *Clinically Oriented Anatomy*, 8th Edition, Publisher Wolters Kluwer, 2018.

[26] Duda R.O., Hart P.E., Stork D.G., *Algorithm-Independent Machine Learning, Pattern Classification*, 2nd Edition, Wiley-Interscience New York, USA, 2000, pp. 531–598.

[27] Park J., Sandberg I.W., *Universal Approximation Using Radial Basis Function Networks*, Neural Computation, **3**(2), 1991, pp. 246–257.

[28] Jang J.S.R., Sun C.T., Mizutani E., *ANFIS: Adaptive Neuro-Fuzzy Inference Systems, Neuro-Fuzzy and Soft Computing: A Computational Approach to Learning and Machine Intelligent*, 1997, Prentice-Hall International, pp. 335–368.

[29] Rissanen J., *Modelling by Shortest Data Description*, Automatica, **14**(5), 1978, pp. 465–471.

[30] Dobrea D.M., Dobrea M.C., *Concepts and Developments of a Wearable System-an IoT Approach*, Proc. IEEE International Symposium on Signals, Circuits and Systems, Iasi, Romania, July 13-14, 2017, pp. 1–4.

[31] Dobrea D.M., Dobrea M.C., *A Neuronal Model of the 3D Head Position Based on a Wearable System*, Proc. IEEE International Conference and Exposition on Electrical and Power Engineering, Iasi, Romania, 2018, pp. 1–6.